Polymorphism of $Ba_{1-x}Sr_xCoO_{3-\delta}$ ($0 \leq x \leq 1$) Perovskites: A Thermal and Structural Study by Neutron Diffraction

Cristina de la Calle[a], José Antonio Alonso[a], and Maria Teresa Fernández-Díaz[b]

[a] Instituto de Ciencia de Materiales de Madrid, CSIC, Cantoblanco, E-28049 Madrid, Spain
[b] Institute Laue-Langevin (ILL) 156X, F-38042 Grenoble Cedex 9, France

Reprint requests to Cristina de la Calle. E-mail: c.delacalle@icmm.csic.es

Dedicated to Professor Gérard Demazeau on the occasion of his 65th birthday

The preparation of different hexagonal, orthorhombic and cubic polymorphs of the solid solution $Ba_{1-x}Sr_xCoO_{3-\delta}$ ($0 \leq x \leq 1$) is described. The samples have been studied by thermal analysis (TG and DTA) to identify the phase transitions; the thermal structural evolution and the structural characterization of different phases were analyzed by X-ray and neutron powder diffraction and refined by the Rietveld method. A series of hexagonal perovskites $Ba_{1-x}Sr_xCoO_{3-\delta}$ ($0 \leq x < 0.5$), labelled as "H", were synthesized by thermal treatment of reactive citrate precursors at 900 °C in high oxygen pressure followed by slow cooling to r. t. The hexagonal perovskites with $0.5 \leq x \leq 1$ were obtained from the citrate precursors heated twice at 900 °C in air and slowly cooled in the furnace. Orthorhombic brownmillerite-like structures, labelled "O", were obtained from precursors with composition $0.5 \leq x \leq 1$ by quenching in liquid N_2 from 900 °C. For $x < 0.5$, quenching from high temperatures does not stabilize the "O" phases. The crystal structure for both terms of the solid solution ($x = 0$ and $x = 1$) has been investigated by neutron powder diffraction. DTA and X-ray thermo-diffractometry show that "H" phases experience a reconstructive transition at *ca.* 900 °C to give cubic "C" polymorphs.

Key words: Neutron Powder Diffraction, Reconstructive Phase Transition, Polymorphism of Cobalt Perovskites, Brownmillerite Structure

Introduction

The cobalt perovskite oxide $SrCoO_{3-\delta}$ and its derivatives have been profusely studied by many authors because of their complex electronic and magnetic properties. An appealing property of this system is the possibility of controlling the oxidation state of cobalt by tuning the concentration of anionic vacancies, with a deep impact on its transport properties. Some of the pioneering work on this system was carried out by Professor G. Demazeau who was interested very early in the different crystallographic phases occurring in this system as a function of temperature and oxygen content [1].

From the beginning, it was clear that the crystal structure of the $SrCoO_{3-\delta}$ perovskites is very sensitive to the preparative conditions. The full oxygen stoichiometry ($\delta = 0$) can be achieved if the synthesis is carried out under high-pressure conditions: $SrCoO_3$ prepared at 6 GPa [2, 3] presents a simple cubic perovskite structure. When $SrCoO_{3-\delta}$ oxides are prepared at ambient pressure conditions, in air atmosphere, they show an approximate stoichiometry $Sr_2Co_2O_5$ (or $SrCoO_{2.5}$) and adopt two very different structural types. In the above-mentioned pioneering work [1] they were classified into two categories, brownmillerite-like structures, so-called "*high-temperature phases*" and hexagonal structures, named "*low-temperature phases*". The stabilization of these structural polymorphs depends on the order-disorder process of the oxygen vacancies. The full ordering of vacancies to give the brownmillerite phase is established in a few seconds during the quenching process after a high-temperature (typically 1000 °C) solid-state synthesis [1, 4, 5]. The brownmillerite structure belongs to the so-called 3C perovskite structural polymorphs, characterized by a 3-dimensional arrangement of corner-sharing polyhedra. The structure of the brownmillerite phase can be derived from the ideal cubic phase by releasing oxygen atoms in an ordered way along the $[110]_{cubic}$ direction [6]. On the other hand, by slow cooling of $SrCoO_{3-\delta}$ samples in air hexago-

nal polymorphs are obtained, with a structure related to that of 2H-$BaNiO_3$ [7], characterized by a face-sharing arrangement of CoO_6 octahedra, as determined by Battle *et al.* [8 – 10]. The scenario is still more complex, as it was demonstrated that samples annealed at low temperature (below 800 °C) did not crystallize in a 2H-type structure with ratio Sr : Co = 1 : 1 but give rise to a cobalt-deficient $Sr_6Co_5O_{15}$ ($SrCo_{0.83}O_{2.5}$) rhombohedral phase [11, 12]. Then, as high-temperature brownmillerite $SrCoO_{2.5}$ cools in air, phase separation into $Sr_6Co_5O_{15}$ and Co_3O_4 occurs [11, 13]. Note that the "*low-temperature*" form of $SrCoO_{2.5}$ previously assigned a 2H-$BaNiO_3$ structure, corresponds to an intergrowth phase [11, 13]. $Sr_6Co_5O_{15}$ was found [13] to be isostructural with $Ba_6Ni_5O_{15}$, as reported by Campá *et al.* [14]. Yamamura *et al.* [15] reported the synthesis, transport and magnetic properties of the Sr-substituted 2H-type solid-solution $Ba_{1-x}Sr_xCoO_{3-\delta}$ ($0 \leq x \leq 0.5$). These authors stated that it is only possible to synthesize the hexagonal Ba-Sr solid solution *via* a precursor route involving the formation of a cubic perovskite. For Sr concentrations greater than $x = 0.5$, the single-phase cubic perovskite-like solid-solution precursor cannot be synthesized, which consequently limits the extent of the Sr content attainable in the 2H-type solid solution. By electron diffraction and high-resolution electron microscopy Boulahya *et al.* [16] identified three 2H-hexagonal perovskite-related $A_{n+2}B'BO_{3n+3}$ phases ($n = 5$, $n = 6$ and $n = 7$).

Grenier *et al.* [1] also studied for $SrCoO_{2.5}$ the relationship between the magnetic behavior and the HS to LS electronic transition, observed in general in Co^{3+} oxides when this cation is in octahedral coordination. At high temperatures there is a sharp drop in susceptibility and, on cooling, susceptibility runs on a different curve, which suggests that the substance has changed from the "*high-temperature phase*" to the "*low-temperature phase*" [17]. The magnetic behavior of the "*low-temperature phase*", which derives from 2H-perovskite, is antiferromagnetic below 25 K, as was reported by Grenier *et al.* in 1979 [1].

In conclusion, $SrCoO_{3-\delta}$ is a material with a surprising structural richness and an important parent compound for the development of series of functional materials. In this work we have investigated some aspects of the tightly related system $Ba_{1-x}Sr_xCoO_{3-\delta}$ ($0 \leq x \leq 1$) in the following way: first we have evaluated the relative stability of the *high-* and *low-temperature polymorphs* by X-ray diffraction (XRD) in order to assess the influence of the quenching tem-

perature on the crystal structure. Our second aim was to determine more precisely the crystal structure of the *low-temperature* polymorphs for $x = 0$ and $x = 1$ by neutron powder diffraction (NPD).

Experimental Section

Synthesis

$Ba_{1-x}Sr_xCoO_{3-\delta}$ ($0 \leq x \leq 1$) materials were obtained in powder form by a citrate technique. Stoichiometric amounts of analytical-grade $Sr(NO_3)_2$, $Ba(NO_3)_2$ and $Co(NO_3)_2 \cdot 6H_2O$ were dissolved in citric acid. The solution was slowly evaporated, leading to a resin which was dried at 120 °C and slowly decomposed at temperatures up to 600 °C for 12 h. For $x < 0.5$, the very reactive precursor powders were subjected to an intermediate treatment at 900 °C in air, in order to favor the oxygenation of the products. Subsequently they were heated at 900 °C under a 200 bar oxygen pressure for 10 h. Finally, the samples were cooled at a rate of 300 °C h^{-1} down to r.t. (*low-temperature phases*). The *low-temperature phase* materials for $x \geq 0.5$ were obtained from the precursors heated twice at 900 °C in air and slowly cooled in air within the furnace. The corresponding *high-temperature phases* ($x \geq 0.5$) were obtained by quenching in liquid N_2 from 900 °C to r.t. These *high-temperature polymorphs* are metastable and cannot be obtained by slow cooling from 900 °C to r.t. In compounds with $x < 0.5$ quenching does not induce this transformation.

X-Ray diffraction

The reaction products were characterized by X-ray diffraction (XRD) for phase identification and to asses phase purity. X-Ray analysis was performed using a Bruker-axstometer (40 kV, 30 mA), controlled by a DIFFRACT^{plus} software, in Bragg-Brentano reflection geometry with CuK_α radiation ($\lambda = 1.5418$ Å). A secondary graphite monochromator allowed the complete removal of CuK_β radiation. The data were obtained between $10 \leq 2\theta \leq 100°$ in steps of 0.05°. The slit system was selected to ensure that the X-ray beam was completely within the sample in all the 2θ range.

An X-ray thermo-diffractometry study was performed with an Anton Parr HTK 1200N temperature vessel. The heating element was made of KANTAL APM (22 % Cr, 5.8 % Al, Fe) and the window of Kapton. The sample was placed in an alumina sample holder which was introduced into the furnace of the diffractometer. The samples were heated in still air from r.t. to 1000 °C at a controlled rate of 10 °C min^{-1}, and cooled again to r.t.

Thermal analysis

Differential thermal analysis (DTA) and thermogravimetric (TG) curves were simultaneously obtained in a Staton

x	0.0	0.1	0.2	0.5	0.7	0.8
a, Å	5.6525(2)	5.6284(7)	5.605(1)	5.6008(2)	5.5598(2)	5.399(4)
c, Å	4.7629(3)	4.7556(7)	4.759(1)	4.3344(1)	4.2774(2)	4.2425(4)
V, Å^3	131.788(7)	130.467(7)	129.479(7)	117.749(5)	114.506(8)	112.759(8)
R_{Bragg}, %	6.2	7.3	12.1	9.8	15.9	17.8

Atom positions: Ba, Sr 2d (1/3, 1/3, 1/3); Co 2a (0, 0, 0); O 6h (x, $-x$, 1/4)

x	0.0	0.1	0.2	0.5	0.7	0.8
x(O)position	0.1502(1)	0.156(2)	0.160(2)	0.152(2)	0.161(2)	0.174(3)

x	0.0	0.1	0.2	0.5	0.7	0.8
(Ba,Sr)–O ($\times$6)	2.979(6)	2.939(8)	2.9166(5)	2.80(1)	2.667(8)	2.61(1)
(Ba,Sr)–O ($\times$6)	2.831(8)	2.82(1)	2.8034(6)	2.790(8)	2.78(1)	2.77(2)
Co–O ($\times$6)	1.895(7)	1.931(8)	1.9535(3)	1.831(9)	1.94(1)	1.98(1)
Co–Co	2.3814(1)	2.3778(4)	2.3794(7)	2.1672(1)	2.1387(1)	2.1213(2)
Co–O–Co	77.8(3)	76.0(4)	75.04(2)	72.6(4)	66.9(5)	64.8(8)

Table 1. Unit-cell parameters, atomic positions, main distances (Å) and selected angles (deg) for the compounds Ba$_{1-x}$Sr$_x$CoO$_{3-\delta}$ ($0 \le x < 1$) after Rietveld refinement from XRD data in the hexagonal space group $P6_3/mmc$ (no. 194). Reliability factors are also given.

STA 781 instrument. The temperatures of the peaks were measured with an accuracy of ± 1 ℃. Analyses were carried out in still air at 10 ℃ min^{-1} heating/cooling rate. The sample and reference (α-Al$_2$O$_3$) were situated in platinum crucibles.

Neutron powder diffraction analysis

Neutron powder diffraction (NPD) diagrams were collected at the Institut Laue-Langevin, Grenoble (France). For the $x = 1$ phase SrCoO$_{3-\delta}$ (*low temperature-phase*), the diffraction patterns were recorded at the high-resolution D2B diffractometer with $\lambda = 1.594$ Å, at 295 K and at 5 K in the angular range $10 \le 2\theta \le 156°$ with 0.05° steps. For the $x = 0$ phase, BaCoO$_3$, the NPD pattern at r. t. was collected at the D2B diffractometer with $\lambda = 1.2316$ Å. NPD diffraction patterns were analyzed by the Rietveld method [18], using the FULLPROF refinement program [19]. A pseudo-Voigt function was chosen to generate the line shape of the diffraction peaks. The coherent scattering lengths for Ba, Sr, Co and O were: 5.070, 7.020, 2.490 and 5.803 fm respectively. The following parameters were refined in the final run: scale factor, background coefficients, zero-point error, pseudo-Voigt corrected for asymmetry parameters, positional coordinates and isotropic thermal factors.

Results

X-Ray diffraction and thermal analysis (DTA-TG)

Fig. 1 shows the evolution of the XRD patterns of Ba$_{1-x}$Sr$_x$CoO$_{3-\delta}$ ($0 \le x \le 1$) as a function of x for the "*low-temperature phases*", which we will call hereafter "H", hexagonal phases. Table 1 includes the unit-cell parameters, main distances and selected angles of the different compounds, after the Rietveld refinements in $P6_3/mmc$ (no. 194) from XRD data. For $x < 0.5$, the refinement is reasonably good in this space group;
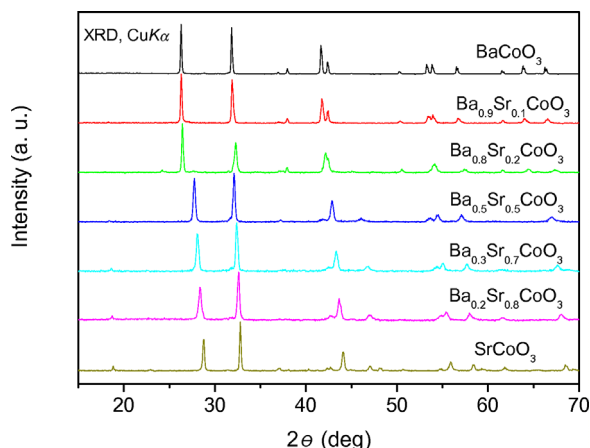

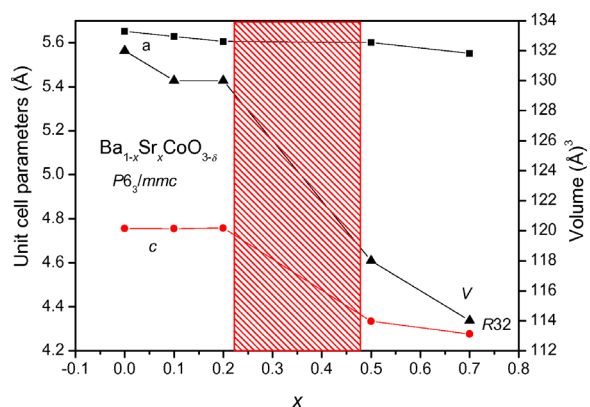Fig. 1. XRD patterns of Ba$_{1-x}$Sr$_x$CoO$_{3-\delta}$ ($0 \le x \le 1$) hexagonal phases.

Fig. 2. Dependence of unit-cell parameters of the x parameter for Ba$_{1-x}$Sr$_x$CoO$_{3-\delta}$ phases, refined in the space group $P6_3/mmc$ from XRD data.

for $x > 0.5$, the sensitivity of X-rays to oxygen positions is not sufficient to show significant differences
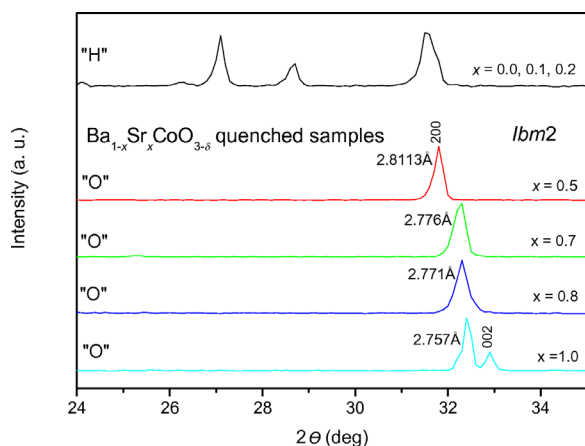
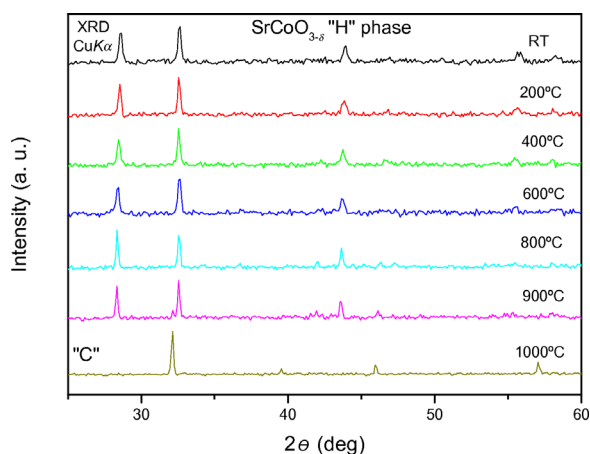Fig. 3. XRD patterns of $Ba_{1-x}Sr_xCoO_{3-\delta}$ $(0 \leq x \leq 1)$ quenched phases.

Fig. 4. Thermo-X-ray diffraction evolution for the $SrCoO_{3-\delta}$ "H" hexagonal phase.

with trial refinements in the trigonal space group $R32$ (no. 155), which was demonstrated to be the correct space group from NPD data. The evolution of the a, c and V parameters is shown in Fig. 2. The abrupt shrinkage observed both in the c parameter and the volume is certainly related to the change of the space group symmetry between Ba-rich ($P6_3/mmc$) and Sr-rich ($R32$) samples, as it will be described below for both end terms of the series, studied by neutron diffraction. Fig. 3 shows the XRD patterns for the equivalent compositions of the "*high-temperature phases*", which we will call hereafter "O", orthorhombic brownmillerite-type phases. These "O" phases can only be stabilized in the compositional range $0.5 \leq x \leq 1$. For $x < 0.5$, the quenching process does not lead to "O" structures.
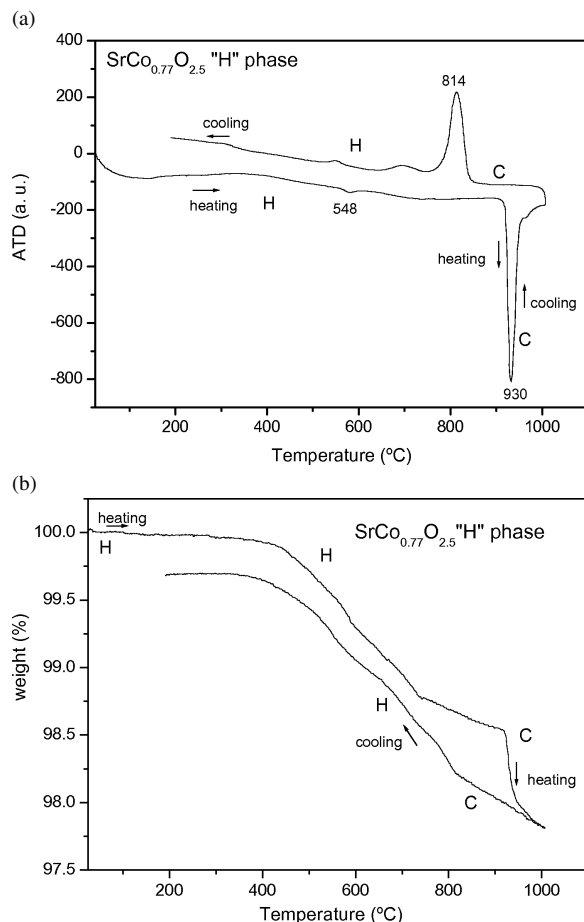

Fig. 5. DTA and TG curves for the $SrCoO_{3-\delta}$ "H" hexagonal phase.

Fig. 3 shows the displacement of the *200* reflection for the "O" phases, corresponding to the evolution of the a parameter from 5.626 Å ($x = 0.5$) to 5.514 Å ($x = 1.0$) along the series. The upper diagram represents the characteristic XRD pattern of the "unquenchable" phases for $x = 0, 0.1, 0.2$.

Thermo-X-ray diffraction studies were performed in still air for "H" $SrCoO_{3-\delta}$ phases from r.t. to 1000 °C and revealed several structural transformations (Fig. 4), in agreement with the results obtained by DTA-TG, as shown in Fig. 5. The "H" $SrCoO_{3-\delta}$ phase transforms at 930 °C to a cubic perovskite, hereafter "C"; this transformation is endothermic and, on cooling, the "C" phase remains until 814 °C. "H" phases are thermodynamically more stables than "O" polymorphs, which are metastable and can only be isolated by quenching. Both "C" and "H" phases
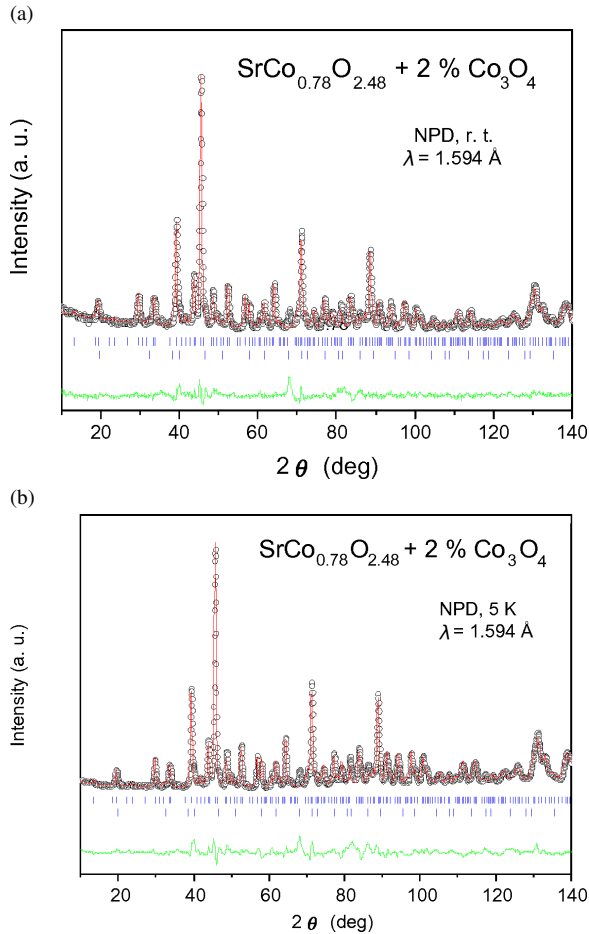
(a)

(b)

Fig. 6. NPD refined pattern for the $SrCoO_{3-\delta}$ "H" phase at (a) r. t. and (b) 5 K.

transform into an "O" polymorph if they are quenched in liquid N_2 from high temperature, typically $900-1200\,°C$. Fig. 5b shows a weight loss of 2.25 % up to $1000\,°C$, equivalent to 0.26 oxygen atoms. This loss is virtually reversible on cooling, recovering the initial mass.

Neutron diffraction

We have collected NPD data for the end values of the $Ba_{1-x}Sr_xCoO_{3-\delta}$ series, $x = 0$ and $x = 1$. For $BaCoO_{3-\delta}$ a diagram at r. t. was collected, whereas for the "H" phase $SrCoO_{3-\delta}$ we recorded high-resolution patterns at r. t. and 5 K.

$SrCoO_{3-\delta}$, "H" polymorph, $Ba_6Ni_5O_{15}$-like

The crystal structure of $SrCoO_{3-\delta}$ was refined by Rietveld methods on the NPD data starting from the

Table 2. Structural parameters for $SrCo_{0.78(1)}O_{2.48(2)}$ ("H" phase) after the Rietveld refinement from NPD data at r. t. and 5 K in the trigonal space group $R32$.

T (K)	298	5
Sr1 $9e$ (x, 0, 1/2):		
x	0.6439(6)	0.6437(5)
B, Å^2	1.7(1)	1.3(1)
Sr2 $9d$ (x, 0, 0):		
x	0.3226(5)	0.3210(5)
B, Å^2	1.2(1)	1.1(1)
Co1 $3b$ (0, 0, 1/2):		
B, Å^2	2.0(9)	0.1(8)
f_{occ}	0.68(7)	0.68(7)
Co2 $6c$ (0, 0, z):		
z	0.102(2)	0.103(1)
B, Å^2	0.3(3)	0.6(4)
Co3 $6c$ (0, 0, z):		
z	0.295(1)	0.296(1)
B, Å^2	0.7(3)	0.5(3)
O1 $9d$ (x, 0, 0):		
x	0.843(1)	0.8436(9)
B, Å^2	1.2(1)	0.3(1)
O2 $18f$ (x, y, z:):		
x	0.4930(6)	0.4946(7)
y	0.6730(6)	0.6728(7)
z	0.4771(3)	0.4785(3)
B, Å^2	0.41(7)	0.22(9)
f_{occ}	0.98(2)	0.98(2)
O3 $18f$ (x, y, z):		
x	0.8436(6)	0.8436(5)
y	−0.0255(6)	−0.0240(5)
z	0.6080(3)	0.6088(3)
B, Å^2	2.4(1)	1.6(1)
χ^2	1.00	1.70
R_p, %	3.59	4.67
R_{wp}, %	4.73	6.33
R_{Bragg}, %	7.1 %	7.9 %
a, Å	9.5008(1)	9.4739(1)
c, Å	12.386(1)	12.360(1)
V, Å^3	968.3(1)	960.8(1)

model defined by Harrison *et al.* [13]. It contains two strontium, three cobalt and three oxygen atoms in the asymmetric unit. The refinement of the occupancy factor for the Co atoms leads to a significant reduction of its contents for Co1, whereas Co2 and Co3 remained stoichiometric. The oxygen occupancy was slightly deficient for O2, and fully stoichiometric for O1 and O3. The refined crystallographic formula was $SrCo_{0.78(1)}O_{2.48(2)}$. According to this formula, the average oxidation state for Co is 3.79(1)+. Figs. 6a and 6b show a good fit of the observed and the calculated profiles in space group $R32$ (no. 155), $Z = 3$, at r. t. and at 5 K, respectively. Table 2 lists the structural

Table 3. Main interatomic distances (Å) and selected angles (deg) for SrCo$_{0.78(1)}$O$_{2.48(2)}$ ("H" phase) as determined by NPD at 298 K and 5 K.

T	298 K	5 K
Sr1–O1 ($\times 2$)	2.602(2)	2.596(2)
Sr1–O2 ($\times 2$)	2.707(5)	2.618(8)
Sr1–O2 ($\times 2$)	2.631(7)	2.700(5)
Sr1–O3 ($\times 2$)	2.430(8)	2.424(6)
$\langle$Sr1–O$\rangle$	2.592(2)	2.584(2)
Sr2–O1 ($\times 2$)	2.655(9)	2.634(9)
Sr2–O2 ($\times 2$)	2.829(5)	2.790(6)
Sr2–O2 ($\times 2$)	2.488(5)	2.488(5)
Sr2–O3 ($\times 2$)	3.130(7)	3.120(6)
Sr2–O3 ($\times 2$)	2.654(5)	2.656(4)
$\langle$Sr2–O$\rangle$	2.751(2)	2.738(2)
Co1–O3 ($\times 6$)	1.922(5)	1.928(5)
$\langle$Co1–O$\rangle$	1.922(2)	1.928(1)
Co2–O1 ($\times 3$)	1.95(1)	1.95(1)
Co2–O2 ($\times 3$)	1.83(1)	1.82(1)
$\langle$Co2–O$\rangle$	1.896(6)	1.892(5)
Co3–O2 ($\times 3$)	1.98(1)	2.02(1)
Co3–O3 ($\times 3$)	1.82(1)	1.81(1)
$\langle$Co3–O$\rangle$	1.905(6)	1.910(5)
Co2–O1–Co2	81(1)	82(1)
Co2–O2–Co3	77(1)	77(1)
Co2–O3–Co3	85(1)	84.6(8)

parameters and atomic positions, and Table 3 includes the main distances and selected angles. The presence of Co$_3$O$_4$, segregated from the main phase during the synthesis process, was quantified to 2 %.

Both Sr atoms are 8-fold coordinated by O atoms ($\langle$Sr1–O$\rangle$ = 2.592(2) Å, $\langle$Sr2–O$\rangle$ = 2.751(2) Å) in an irregular coordination. The atoms Sr1 and Sr2 are disposed in columns running parallel to the *c* direction. Two cobalt atoms, Co2 and Co3 (site 6*c*), are octahedrally coordinated by oxygen atoms ($\langle$Co2–O$\rangle$ = 1.896(6) Å, $\langle$Co3–O$\rangle$ = 1.905(6) Å), and the third, Co1 (site 3*b*), occupies a distorted trigonal antiprism ($\langle$Co1–O$\rangle$ = 1.922(2) Å and O–Co1–O = 76.8(4)°). The crystal structure consists of isolated, infinite chains of face-sharing CoO$_6$ polyhedra running along the *c* direction. The repeat unit for Co–O species consists of four distorted octahedra sharing faces intermingled with prismatically-coordinated Co1 atoms. The inter-octahedral cobalt–cobalt distances are Co2–Co3 = 2.39(3) Å and Co2–Co2 = 2.54(3) Å. The face-sharing prismatic/octahedral Co1–Co3 distance is 2.53(2) Å. These results are comparable with those obtained by Harrison *et al.* [13] for the phase Sr$_6$Co$_5$O$_{15}$, although in our case we deal with a more severely Co-deficient compound, with a slightly smaller cell volume of 968.3 Å^3 (969.6 Å^3

for Sr$_6$Co$_5$O$_{15}$ [13]), corresponding to a higher average oxidation state for the Co cations.

The crystal structure is maintained at low temperature (5 K), showing the corresponding contraction of unit cell parameters and bond lengths. No ordering of the magnetic moments of Co was observed on the 5 K NPD pattern. This hexagonal phase was reported as paramagnetic in a wide range of temperature [1]; the magnetic order described by Grenier *et al.* [1] at low temperature (T_N = 25 K) can be related in our opinion to the presence of Co$_3$O$_4$ segregated from the main phase. The magnetic behavior of "H" Sr$_2$Co$_2$O$_5$, considered stoichiometric by these authors and derived from the 2H-BaNiO$_3$ structure, is explained by the simultaneous presence of IS ($t_{2g}^5 e_g^1$) and LS (t_{2g}^6) states of trivalent Co [1].

BaCoO$_3$, "H" polymorph, BaNiO$_3$-like

The crystal structure was refined from NPD data collected at r. t. (λ = 1.2316 Å) in the hexagonal space group $P6_3/mmc$ (no. 194). The lattice parameters were a = 5.6472(2), c = 4.7582(2) Å and V = 131.41(0) Å^3. Ba, Co and O atoms were located at the 2*d*, 2*a* and 6*h* positions, respectively. A good fit of the observed and the calculated profiles was obtained, as shown in Fig. 7. Table 4 lists the refined unit cell, structural and thermal parameters, and includes the mean interatomic distances and some selected bond angles. A refinement of the occupations in the positions of Co and O allowed us to establish the crystallographic formula to BaCo$_{0.998(5)}$O$_{2.782(2)}$.

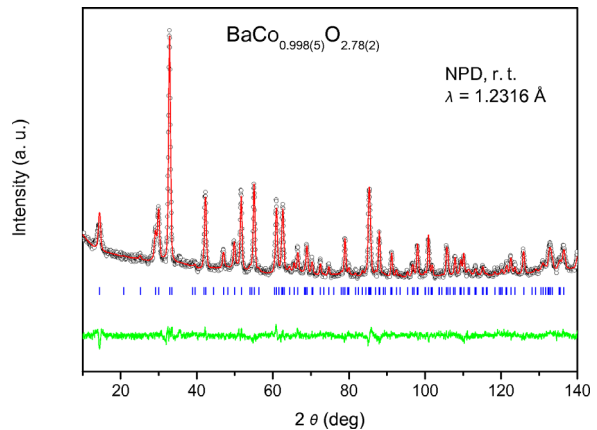Fig. 8 displays a view of the BaCoO$_3$ 2-H structure, containing chains of CoO$_6$ octahedra sharing

Fig. 7. NPD refined pattern for the BaCoO$_{3-\delta}$ "H" phase at r. t.

Table 4. Structural parameters, main interatomic distances (Å) and selected angles (deg) for the $BaCoO_3$ phase after Rietveld refinement of NPD data at r. t. in the hexagonal space group $P6_3/mmc$; $a = 5.6472(2)$; $c = 4.7582(2)$ Å; $V = 131.4(1)$ Å^3; reliability factors are given in parentheses[a].

Atom	site	x	y	z	$B(Å^2)$	f_{occ}	Distances (Å) and angles (deg)		
Ba	$2d$	1/3	2/3	3/4	1.19(6)	0.0833	Ba–O (×6)	2.9780(4)	Co–O (×6)	1.8905(2)
Co	$2a$	0	0	0	1.13(9)	0.0832(5)	Ba–O (×6)	2.8282(8)	Co–Co (×2)	2.3792(1)
O	$6h$	0.1502(1)	−0.1502(1)	1/4	1.06(2)	0.232(2)	⟨Ba–O⟩	2.9031(2)	Co–O–Co	77.98(2)

[a] $\chi^2 = 0.56$, $R_p = 3.53\%$, $R_{wp} = 4.51\%$, $R_{exp} = 5.99\%$, $R_{Bragg} = 9.2\%$.
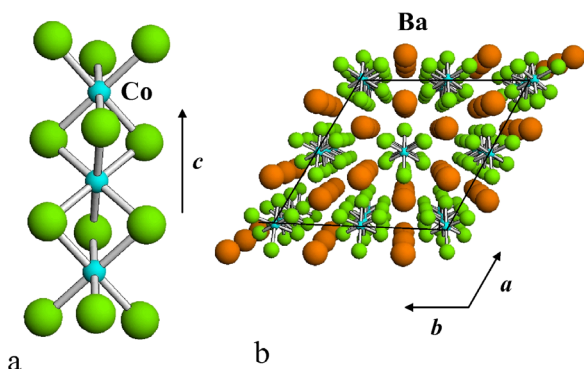

Fig. 8. Two views of the crystal structure of $BaCoO_3$ showing (a) an individual chain of CoO_6 octahedra sharing faces along the *c* axis and (b) a projection of the crystal structure onto the *ab* plane.

faces along the *c* axis. As shown in Table 4, Ba–O distances in the BaO_{12} polyhedron display an average ⟨Ba–O⟩ bond length of 2.90 Å which compares well with that expected from the sum of the ionic radii [20] of 3.01 Å for $^{XII}Ba^{2+}$ (1.61 Å) and $^{VI}O^{2-}$ (1.40 Å). Co–Co distances of *ca.* 2.38 Å are indicative of face-sharing CoO_6 octahedra. For the Co–O bonds the average length of 1.89 Å is in good agreement with the 1.93 Å expected for $^{VI}Co^{4+}$ ions (0.53 Å).

Discussion and Conclusion

The $Ba_{1-x}Sr_xCoO_{3-\delta}$ system is very rich in structural variations; several structural transitions can be induced either by changing the *x* value, by increasing the temperature from r. t. or by quenching the sample at the end of the synthetic process. It has been shown that an "O" brownmillerite-like structure can be obtained only by quenching the precursors with initial compositions $x \geq 0.5$. It is well known that the metastable brownmillerite phase is formed within a very short time during the quenching process by ordering of the oxygen vacancies. The fact that the Ba-rich samples cannot be

stabilized as "O" phases for $x > 0.5$ is certainly related to the tolerance factor of the perovskite, linked with the much larger ionic radius of Ba^{2+} (1.61 Å) as compared to Sr^{2+} (1.44 Å). Above a critical tolerance factor it is not possible to stabilize perovskite structures containing a corner-sharing arrangement of octahedra, giving rise to face-sharing octahedral networks with hexagonal symmetry. The influence of the tolerance factor is also evident in the structural evolution with the *x* value for the "H" hexagonal phases, obtained by slow cooling in air of the precursors. A 2H-hexagonal phase ($BaNiO_3$-type) is obtained for large tolerance factors, $x < 0.5$, but more complex distorted hexagonal structures *n*H-hexagonal, showing trigonal symmetry, are observed for $x \geq 0.5$, many of which correspond to intergrowth phases, the structural refinement of which requires the help of other techniques such as electron microscopy [17].

Yamamura *et al.* [15] reported the synthesis of a partial region of the $Ba_{1-x}Sr_xCoO_{3-\delta}$ ($0 \leq x \leq 0.5$) solid solution, utilizing an indirect synthesis procedure involving the preliminary formation of a cubic perovskite. In the present work, we found an access to different members of the solid solution within the entire compositional regime ($0 \leq x \leq 1.0$) starting from very reactive citrate precursors, slowly cooled in air from 900 °C. It is noteworthy that the slow cooling treatment of the samples involves a segregation of some Co as Co_3O_4, giving rise to crystal structures with (Ba/Sr)/Co ratios away from unity. In the case of $SrCo_{0.78(1)}O_{2.48(2)}$, refined from NPD data, the amount of crystalline Co_3O_4, introduced as a second phase during the refinement, is only 2%, much lower than that expected from the final stoichiometry of the main phase, $SrCo_{0.78(1)}O_{2.48(2)}$, where 22% of Co is missing from the initial Sr/Co= 1 : 1 ratio. Most probably, a large amount of segregated Co is in an amorphous phase, or with small particle size, not visible by diffraction methods. It is clear that the missing Co is not lost during the synthesis process, since the 1 : 1 stoichiom-

etry can be recovered by quenching the "H" sample in liquid N$_2$ from high temperature.

Finally, it is worth pointing out that the thermal evolution of the crystal structure of "H" phases, observed *in situ* by X-ray diffractometry complemented by DTA measurements, leads to "C" cubic, oxygen-deficient phases, by heating in air at temperatures above 900 °C (1173 K). Actually, this cubic phase corresponds to the so-called "stable orthorhombic" phase described in the pioneering work by Grenier *et al.* [1], tightly linked to a Co spin transition from an IS to a HS state. It is well known that the spin state depends on the strength of the crystal field experienced by Co^{3+} in octahedral coordination. The HS state ($t_{2g}^4 e_g^2$) is achieved in weak octahedral ligand fields, whereas the LS state (t_{2g}^6) occurs in strong fields, for instance it is often observed in complex fluorides. The IS state ($t_{2g}^5 e_g^1$) can be the ground state in lower symmetries like axially distorted octahedra [21]. This is the case in the "H" phase, where the presence of axially deformed CoO$_6$ units (octahedra and trigonal antiprisms) certainly favors the IS configuration for Co. The final transition, above 930 °C for $x = 1$, to a cubic phase with a corner-linked octahedral arrangement, characterized by a lower octahedral field, is concomitant with the increase in susceptibility reported by Grenier *et al.* [1] concurrent with the magnetic transition to a HS state.

[1] J. G. Grenier, S. Ghodbane, G. Demazeau, M. Pouchard, P. Hagenmuller, *Mat. Res. Bull.* **1979**, *14*, 831.

[2] X. L. Wang, H. Sakurai, E. Takayama-Muromachi, *J. Appl. Phys.* **2005**, *97*, 10M519.

[3] Z. Q. Deng, W. S. Yang, W. Liu, C. S. Chen, *J. Solid State Chem.* **2006**, *179*, 362.

[4] H. Watanabe, T. Takeda, *Proc. Int. Conf. on Ferrites*, Japan **1970**, p. 598.

[5] J. Rodríguez, J. M. González-Calbet, J. C. Grenier, J. Pannetier, M. Anne, *Solid State Commun.* **1987**, *62*, 231.

[6] R. Le Tocquin, W. Paulus, A. Cousson, C. Prestipino, C. Lamberti, *J. Amer. Chem. Soc.* **2006**, *128*, 40, 13161.

[7] J. C. Grenier, L. Fournés, M. Pouchard, P. Hagenmuller, *Mater. Res. Bull.* **1986**, *21*, 441.

[8] P. D. Battle, T. C. Gibb, A. T. Steel, *J. Chem. Soc., Dalton Trans.* **1987**, 2359.

[9] P. D. Battle, T. C. Gibb, *J. Chem. Soc., Dalton Trans.* **1987**, 667.

[10] P. D. Battle, T. C. Gibb, A. T. Steel, *J. Chem. Soc., Dalton Trans.* **1988**, 83.

[11] Y. Takeda, R. Kanno, T. Takada, O. Yamamoto, M. Takano, Y. Bando, *Z. Anorg. Allg. Chem.* **1986**, *540-541*, 259.

[12] J. Rodríguez, J. M. González-Calbet, *Mater. Res. Bull.* **1986**, *21*, 429.

[13] W. Harrison, S. L. Hedwood, A. J. Jacobson, *J. Chem. Soc., Chem. Commun.* **1995**, 1953.

[14] J. A. Campá, E. Gutiérrez-Puebla, M. A. Monge, I. Rasines, C. Ruiz-Valero, *J. Solid State Chem.* **1994**, *108*, 230.

[15] K. Yamamura, H. W. Zandbergen, K. Abe, R. J. Cava, *J. Solid State Chem.* **1999**, *146*, 96.

[16] K. Boulahya, M. Parras, J. M. González-Calbet, *J. Solid State Chem.* **1999**, *142*, 419.

[17] T. Takeda, H. Watanabe, *J. Phys. Soc. Jpn.* **1972**, *33*, 973.

[18] H. M. Rietveld, *J. Appl. Crystallogr.* **1969**, *2*, 65.

[19] J. Rodríguez-Carvajal, *Physica B* **1993**, *192*, 55.

[20] R. D. Shannnon, *Acta Crystallogr.* **1976**, *A 32*, 751.

[21] B. Buffat, G. Demazeau, M. Pouchard, P. Hagenmuller, *Proc. Indian Acad. Sci.* **1984**, *93*, 313.